

Distribution Agreement

In presenting this thesis as a partial fulfillment of the requirements for a degree from Emory University, I hereby grant to Emory University and its agents the non-exclusive license to archive, make accessible, and display my thesis in whole or in part in all forms of media, now or hereafter now, including display on the World Wide Web. I understand that I may select some access restrictions as part of the online submission of this thesis. I retain all ownership rights to the copyright of the thesis. I also retain the right to use in future works (such as articles or books) all or part of this thesis.

Parisa Keshavarz-Joud

March 27, 2018

Engineering the Regioselectivity of Cyclododecanone Monooxygenase

by

Parisa Keshavarz-Joud

Dr. Stefan Lutz
Adviser

Emory College Chemistry Department

Dr. Stefan Lutz
Adviser

Dr. Emily Weinert
Committee Member

Dr. Christine Dunham
Committee Member

2018

Engineering the Regioselectivity of Cyclododecanone Monooxygenase

By

Parisa Keshavarz-Joud

Dr. Stefan Lutz

Adviser

An abstract of
a thesis submitted to the Faculty of Emory College of Arts and Sciences
of Emory University in partial fulfillment
of the requirements of the degree of
Bachelor of Sciences with Honors

Department of Chemistry

2018

Abstract

Engineering the Regioselectivity of Cyclododecanone Monooxygenase

By Parisa Keshavarz-Joud

Baeyer-Villiger monooxygenases (BVMOs) are the enzymatic alternatives to the chemical Baeyer-Villiger oxidation reaction. The regioselectivity of these enzymes is mostly dependent upon active site residues that govern the stability of the Criegee intermediate and the preferred migratory group of the substrate. The BVMO of interest in this work is cyclododecanone monooxygenase from *Rhodococcus ruber* SC1 (CDMO). We aim to achieve higher regioselectivity towards two substrates, methyl (2-methyl-6-oxooctan-4-yl) carbamate and 3-methylcyclohexanone. The unnatural product formed as the result of Baeyer-Villiger oxidation with methyl (2-methyl-6-oxooctan-4-yl) carbamate is a β -amino acid ester, which after hydrolysis yields useful building blocks for the production of β -peptides, alkaloids, and β -lactam antibiotics. As indicated in literature sources, the conserved arginine-interacting loop in the structure of some BVMOs plays an important role in directing product regioselectivity. We were able to increase the size of the CDMO active site via rational engineering by truncating amino acid side chains on the above-mentioned loop. Here we introduce novel variants with increased activity and regioselectivity towards methyl (2-methyl-6-oxooctan-4-yl) carbamate that also form the unnatural product. Furthermore, we demonstrated that the observed change in regioselectivity does not apply universally, as seen with 3-methylcyclohexanone. Neither of the constructed variants showed promising conversion rates or increased regioselectivity towards 3-methylcyclohexanone and it is potentially due to its small size compared to methyl (2-methyl-6-oxooctan-4-yl) carbamate.

Engineering the Regioselectivity of Cyclododecanone Monooxygenase

By

Parisa Keshavarz-Joud

Dr. Stefan Lutz

Adviser

A thesis submitted to the Faculty of Emory College of Arts and Sciences
of Emory University in partial fulfillment
of the requirements of the degree of
Bachelor of Sciences with Honors

Department of Chemistry

2018

Acknowledgements

I would like to thank my wonderful mentor, Dr. Leann Q. Teadt, who sacrificed so much of her time to teach me everything I know about protein engineering. She helped me learn from my mistakes, understand the fundamental science behind the techniques, and frankly, become a chemist. I would not have been able to go through the Honors Thesis Program without her guidance, support, and passion for teaching.

I would also like to thank the current members of Lutz lab who helped me write this thesis and made my experience in the lab joyful: Samantha Iamurri, Matthew Jenkins, Dr. Huanyu Zhao, Dr. Elsie Williams, David White, Evy Kimbrough, and my fellow undergraduates Angel Gonzalez-Valero and Michelle Jung. I also appreciate my thesis committee members, Dr. Emily Weinert and Dr. Christine Dunham, for being a part of this process.

My academic career changed for better the day Dr. Stefan Lutz offered me a position in his lab. Dr. Lutz made me passionate about biochemistry and gave me the opportunity to experience research in this area. I truly appreciate the support, advice, and the time he has given me.

Most of all, I would like to thank my family for always believing in me. Their continuous support, love, and encouragements made it possible for me to be where I am today. There are not enough words for me to express how grateful I am for all they have done. I am incredibly lucky to have them.

Table of Contents

1. Introduction.....	1
1.1. Baeyer-Villiger Oxidation	1
1.2. Baeyer Villiger Monooxygenases (BVMOs).....	4
1.2.1. Arginine-Interacting Loop	6
1.2.2. Cyclododecanone Monooxygenase	7
2. Materials and Methods.....	11
2.1. Cloning.....	11
2.2. Expression.....	12
2.3. Purification.....	13
2.4. Activity Assay.....	14
2.5. GC Protocol	15
2.6. GCMS Protocol.....	15
3. Results and Discussion	16
3.1. Loop Mutations	16
3.2. Variants P190I/A498G and P190I/L499G.....	21
4. Conclusion	27
5. References.....	29

Table of Figures and Schemes

Scheme 1.....	1
Scheme 2.....	3
Figure 1.....	5
Figure 2.....	9
Scheme 3.....	10
Scheme 4.....	10
Figure 3.....	16
Figure 4.....	19
Figure 5.....	20
Figure 6.....	24
Figure 7.....	24
Figure 8.....	26
Figure 9.....	28

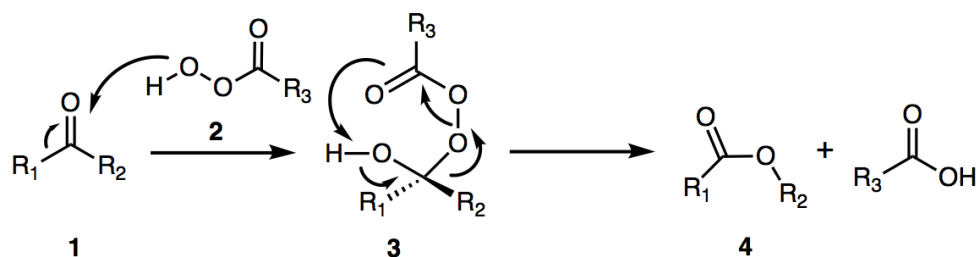
Table of Tables

Table 1.....	12
Table 2.....	12
Table 3.....	15
Table 4.....	17
Table 5.....	18
Table 6.....	22
Table 7.....	23

1. Introduction

1.1. Baeyer-Villiger Oxidation

Baeyer-Villiger oxidation is a key reaction in synthetic chemistry for the insertion of an oxygen atom adjacent to a carbonyl group¹. This reaction has been used over the past century to create novel biological pathways and synthesize new molecules¹. For example, Baeyer-Villiger oxidation was employed to transform steroids to novel molecules that can potentially modulate estrogen balance in the nature². Peracids are used in this reaction to allow the conversion of ketones to esters or cyclic ketones to lactones³. Rudolf Criegee proposed a two-step process for this reaction as shown in Scheme 1⁴⁻⁵. The first step involves nucleophilic attack on the carbonyl group (1) by peracid (2), which results in the formation of a “Criegee” intermediate (3)⁴⁻⁵. During the second step, the rearrangement of the intermediate results in the production of the corresponding ester (4) or lactone⁵. If $R_1 \neq R_2$, the reaction can produce two possible regioisomers¹. Preference in regard to regioselectivity depends on the migratory aptitude of the R-groups flanking the carbonyl carbon and stability of the carbocation transiently formed in the intermediate step⁶. The preferred migration is to the R group with the higher degree of substitution¹. For example, R groups containing secondary and tertiary carbons are favored over a primary carbon¹. For this reason, control over regioselectivity is limited and production of the unnatural isomer is not possible through the traditional chemical Baeyer-Villiger oxidation⁵.



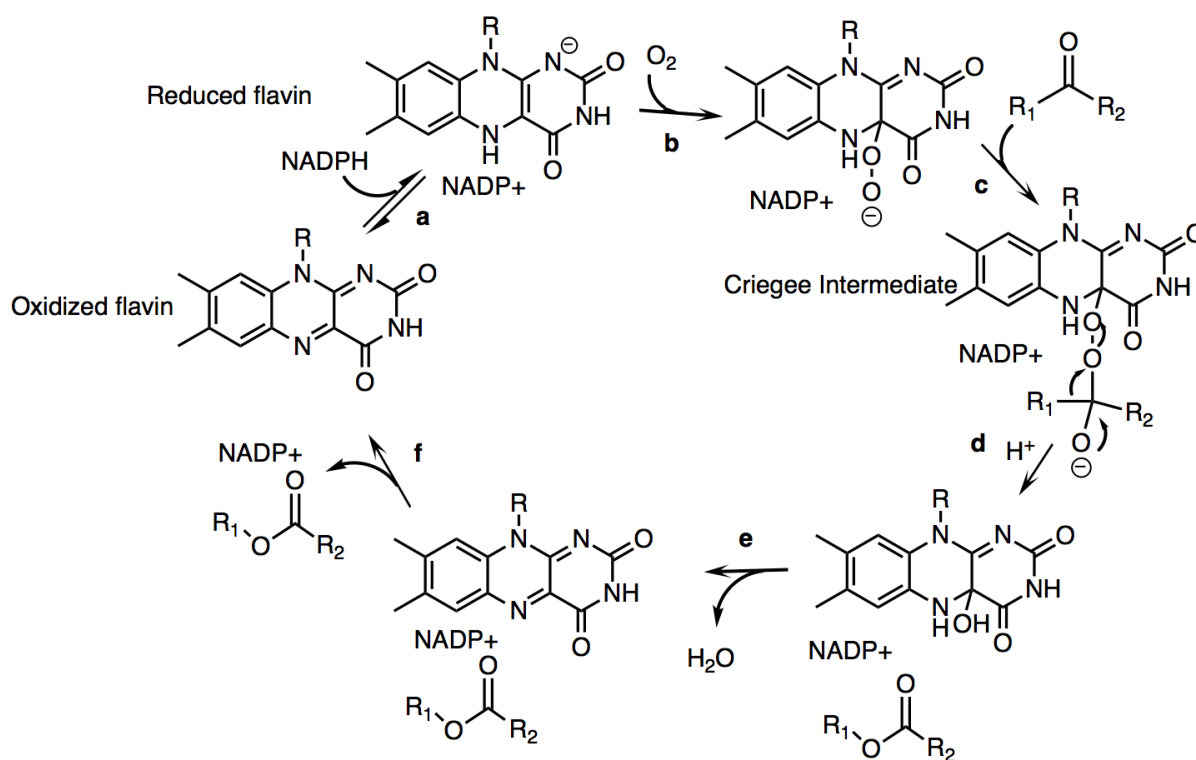
Scheme 1: Baeyer-Villiger Oxidation Reaction (figure adapted from Leisch, H.; Morley, K.; Lau, P. C. K. *Chemical Reviews* **2011**, *111* (7), 4165-4222⁵.)

Beyond the limited regio-control of chemical Baeyer-Villiger oxidation, the reaction is also not environmentally friendly⁵. Peracids, especially organic peroxides, used in Baeyer-Villiger oxidation reactions are highly reactive, combustible, and thermally unstable substances due to volatile O-O peroxy linkage⁷.

An alternative route for this reaction is the use of Baeyer-Villiger monooxygenases (BVMOs). BVMOs are flavoenzymes that belong to a class of oxidoreductases and provide a “green chemistry” through the use of molecular oxygen instead of peracids⁵. BVMOs usually show excellent regio- and stereo-selectivity which can be beneficial for obtaining a regioisomerically pure product⁸. The active-site of these enzymes are able to overrule the migratory aptitude to form both the naturally and unnaturally occurring regioisomers⁹. This property of the BVMOs can be very useful in industrial and medicinal routes and enables the production of either regioisomer of interest¹⁰. These enzymes use a flavin cofactor, a nicotinamide cofactor, and molecular oxygen to help complete the catalytic cycle¹¹.

Mechanistically, biocatalysis in BVMOs is initiated by reduction of flavin adenine dinucleotide (FAD) by NADPH in the active site (Scheme 2, a)^{9, 11-12}. Subsequently, molecular oxygen binds to the reduced flavin in the C-4 α position to form C-4 α peroxyflavin (b)^{9, 11-12}. This intermediate acts as a nucleophile and attacks the substrate's carbonyl group to create the Criegee intermediate (c)^{4, 9, 11}. The product is then formed following migration of one of the R-groups (d), flavin is oxidized back to its initial state, and water is subsequently released (e)^{9, 11-12}. Finally, NADP⁺ and product are released from the active site of the BVMO (f)¹². The Berghuis group demonstrated the movement of the nicotinamide cofactor as it remains bound in the active site throughout the catalytic cycle¹³. This repositioning allows the reduction of the flavin first and later the stabilization of the Criegee intermediate.¹³ Based on structural and

protein engineering studies, the active site architecture is the primary factor determining which regioisomer is formed. The active site residues can affect the orientation and stability of the Criegee intermediate, thereby preferentially promoting the migration of one R-group over another.⁶ It was previously found that the migrating bond in the Criegee intermediate needs to be antiperiplanar to the oxygen–oxygen bond of the peroxide¹¹. Therefore, the rule of migration based on the highest substituted R group can only be followed when the steric effects in the active site allow the positioning of the substrate in such way¹⁴. As a result, BVMOs can allow the formation of the unnatural regioisomer, which is highly advantageous compared to the chemical Baeyer-Villiger oxidation with peracids⁹.



Scheme 2: Catalytic cycle of BVMOs. (Figure adapted from Mihovilovic, Marko D.; Müller, B.; Stanetty, P. *European Journal of Organic Chemistry* **2002**, 22, 3711-3730¹¹.)

1.2. Baeyer Villiger Monooxygenases (BVMOs)

Interest in BVMOs was first raised with the purification of cyclohexanone monooxygenases from *Nocardia globerula* CL1 and *Acinetobacter* NCIB 9871 by the Trudgill group in 1976¹⁵. Since then, experiments have been conducted to better understand the structure of BVMOs, and also conduct experiments to alter activity, regio- and enantio- selectivity, and substrate preference^{14, 16}.

Structurally, BVMOs are classified into three major categories: Type 1, Type 2, and Type O⁵. Type I includes enzymes with a tightly bound FAD, a fingerprint motif sequence, and Rossmann fold as their structural motif^{5, 11}. Type 2 BVMOs use flavin mononucleotide (FMN) and lack a fingerprint motif⁵. Furthermore, these BVMOs, unlike type 1 and type O, are products of two genetic components, a reductase and an oxygenase⁵. The reductase utilizes NAD(P)H to reduce FMN, while the oxygenase uses the reduced flavin to perform the Baeyer-Villiger reaction⁵. Sequence-wise and structural-wise, Type O BVMOs are different than the other two categories and have not been widely studied⁵. For the purpose of this paper, however, we focus on Type 1 BVMOs as they are closely applicable to the reactions of our interest.

Among the BVMOs selected for protein engineering, cyclohexanone monooxygenases (CHMOs) and phenylacetone monooxygenase (PAMO) have received great attention in previous years^{14, 17}. Of particular note is research by the Bornscheuer group, which aimed to switch the regioselectivity of CHMO from *Arthrobacter* sp. (CHMO_{Arthro})¹⁴. Interestingly, the reaction of the wild-type CHMO_{Arthro} with *trans*-dihydrocarvone favors the production of the regioisomer with the oxygen atom inserted in the less substituted residue (abnormal lactone)¹⁴. The aim of their study was to construct a variant that favors the production of a chemically preferred regioisomer (normal lactone)¹⁴. To estimate the position of active site residues, they relied on a

homology model based on the loose conformation of CHMO from *Rhodococcus sp.* HI-31 (CHMO_{Rhodo}, 84% protein sequence similarity), as shown in Figure 1¹⁴. After testing a number of variants, they discovered that the substitution of F485, F299, and F330 to Ala resulted in a reversal of regioselectivity for *trans*-dihydrocarvone¹⁴. These substitutions contained smaller side chains, and as a result, increased the size of the active site¹⁴. They were also able to alter the regioselectivity of the enzyme by conjugating F299A/F330A with substitution of L196 to Phe¹⁴. Therefore, they concluded that the migratory bond in the Criegee intermediate in these variants was able to position itself in an antiperiplanar way that favored the production of the normal lactone¹⁴.

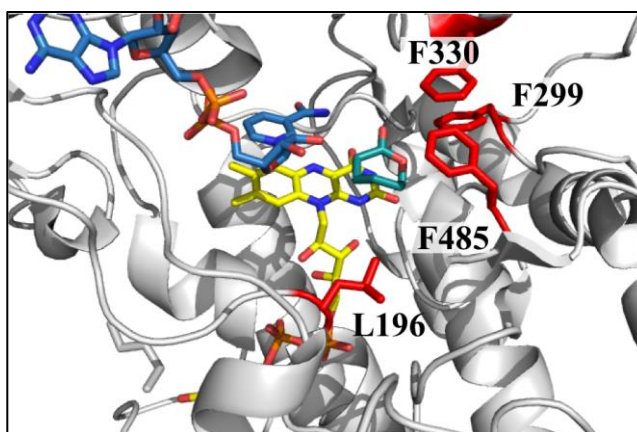


Figure 1: Crystal structure of CHMO_{Rhodo} (loose conformation, PDB 4RG4)¹⁸ used by Bornscheuer group to alter the regioselectivity of CHMO_{Arthro}. The position of L196, F299, F330, and F485 (red) are shown relative to the substrate (caprolactone, green). The substrate's active site is located above isoalloxazine ring of FAD (yellow) in close proximity to the three phenylalanine residues. Additionally, NADP⁺ (blue) is located on the top left side of isoalloxazine ring.

Manfred T. Reetz, a prominent chemical biologist interested in the reactions of BVMOs, has conducted many remarkable research studies on PAMOs¹⁷. In one such study, his group was able to alter the substrate specificity and stereoselectivity of PAMO from *Thermobifida fusca*¹⁷. Similar to the Bornscheuer group, they employed a homology model based on CHMO from *Acinetobacter sp.*, due to the unresolved crystal structure of any CHMO at the time¹⁷. Since the

crystal structure of PAMO had been recently solved, it was discovered upon comparison that its active site is smaller than the active site of CHMO_{Acineto}^{9, 19}. They constructed three variants to enlarge the active site of CHMO_{Acineto}, P1 (deletion of A442), P2 (deletion of A442 and L443), and P3 (deletion of S441 and A442), and tested their activities with 2-phenylcyclohexanone and 2-benzylcyclohexan-1-one¹⁷. They observed increasing conversion rate of 2-phenylcyclohexanone in the order of P1<P2<P3¹⁷. While wild-type PAMO converted only 10% of this substrate after 24 hours, P3 was able to show a conversion rate of 91%¹⁷. In the reactions with 2-benzylcyclohexan-1-one, wild-type PAMO was inactive, and P3 converted 40% of the substrate to the corresponding products after 24 hours¹⁷. Deletions in variants P1, P2, and P3 enlarged the active site and allowed for a better substrate positioning¹⁷. Because the focus of this research was substrate specificity, this group did not report the regioselectivity of these variants towards the substrates tested¹⁷.

1.2.1. Arginine-Interacting Loop

In separate studies, a catalytically relevant arginine has been identified to be conserved in the BVMO family¹⁹. This arginine plays an important role in stabilizing the Criegee intermediate through hydrogen bonding¹⁹. The Reetz group reported the presence of a loop that is believed to interact with the observed arginine and appears to play a role in substrate specificity¹⁷. The residues of the loop, however, are not conserved among the BVMO family²⁰. Different studies have focused on substitution within this loop to determine its effect on the regioselectivity of the enzyme^{14, 20}. In the previously mentioned research by Bornscheuer group, F485 is located on the arginine-interacting loop of CHMO_{Arthro}¹⁴. Furthermore, the group of Reetz^{17, 20} and Fraaije^{16, 21} constructed variants on the homologous loop in PAMO to test its effects on activity and

regioselectivity. The research by the Reetz group that was previously discussed deleted residues from this loop and gained higher activity towards 2-phenylcyclohexanone and 2-benzylcyclohexan-1-one¹⁷. However, it has been shown that increasing the size of the active site does not universally result in higher conversion and regioselectivity but is highly substrate specific²⁰.

1.2.2. Cyclododecanone Monooxygenase

Cyclododecanone monooxygenase from *Rhodococcus ruber* *SCI* (CDMO) is an interesting and useful BVMO due to its relatively large active site^{5, 22}. A successful cloning and expression of CDMO in *E. coli* was first reported by the Cheng group in 2001²³. Compared to CHMOs and PAMO, CDMO is capable of accepting larger substrates, such as long-chain cyclic ketones^{5, 23}. This feature differentiates CDMO from CHMOs, which exhibit specificity towards short-chain cyclic compounds²³. Another interesting feature of CDMO is its high activity towards N-protected β -amino ketones, which are converted into two pharmaceutically important precursors (discussed further below)²². Altering the regioselectivity of this enzyme will be greatly beneficial, as it accepts types of substrates that are not effectively processed by other BVMOs²².

As attempts to crystallize CDMO have so far been unsuccessful, a homology model was constructed to evaluate the key active site residues²⁴. This process initiated with comparing CDMO's protein sequence to BVMOs such as CHMO from *Acinetobacter* NCIMB 9871, CHMO_{Rhodo}, PAMO, and polycyclic ketone monooxygenase (PockeMO) from *Thermothelomyces thermophile*.²⁴ The results suggested that CDMO had the highest sequence identity with PockeMO, with 42% similarity²⁵. Using RaptorX²⁶ and Rosetta Design software²⁷

for the structural prediction, the CDMO homology model was constructed. The protein backbone of the relaxed homology model closely resembles the structure of PockeMO (PDB entry: 5MQ6)²⁵, with the position of a loop near the active site shifted. The position of FAD remained unchanged, while the nicotinamide cofactor rotated by approximately 60° from the active site.²⁴ Additionally, caprolactone represented the substrate in the active site of the homology model (Figure 2).²⁴

The experiments conducted on CHMO_{Arthro} and PAMO proposed that changing the size of the amino acid side chains on the arginine-interacting loop alters the position of the catalytic arginine, and subsequently changes the space provided for the Criegee intermediate to position itself^{14, 17}. This structural change within the enzymes has previously resulted in change in activity and regioselectivity of the enzyme^{14, 17}. Since decreasing the size of the amino acid side chains developed interesting results in both of the research studies from the Bornscheuer and Reetz groups, we aimed to perform similar mutagenesis experiments on the corresponding loop in CDMO to see whether we can achieve higher regioselectivity for any of the substrates (discussed below). The homologous loop in CDMO includes residues A498/L499/G500/S501²⁰. Residues A498 and L499 within the loop were the main focus of my study (Figure 2). Substitutions within the loop were also performed by other members in the lab. Because Ala and Leu have relatively short side chains compared to other amino acids, we either substituted these residues to Gly or deleted them. Four CDMO variants of A498G/L499G, Δ A498L499, A498G, and L499G were initially generated to test with the substrates discussed below. At the time of this analysis, Dr. Leann Teadt was analyzing the effects of amino acid substitutions on different regions of CDMO. A promising variant constructed by her was P190I, which is a homologous residue to L196 from CHMO_{Arthro}. Due to interesting results obtained with A498G and L499G,

these variants were each coupled with P190I to test whether the double variants show enhanced activity and regioselectivity.

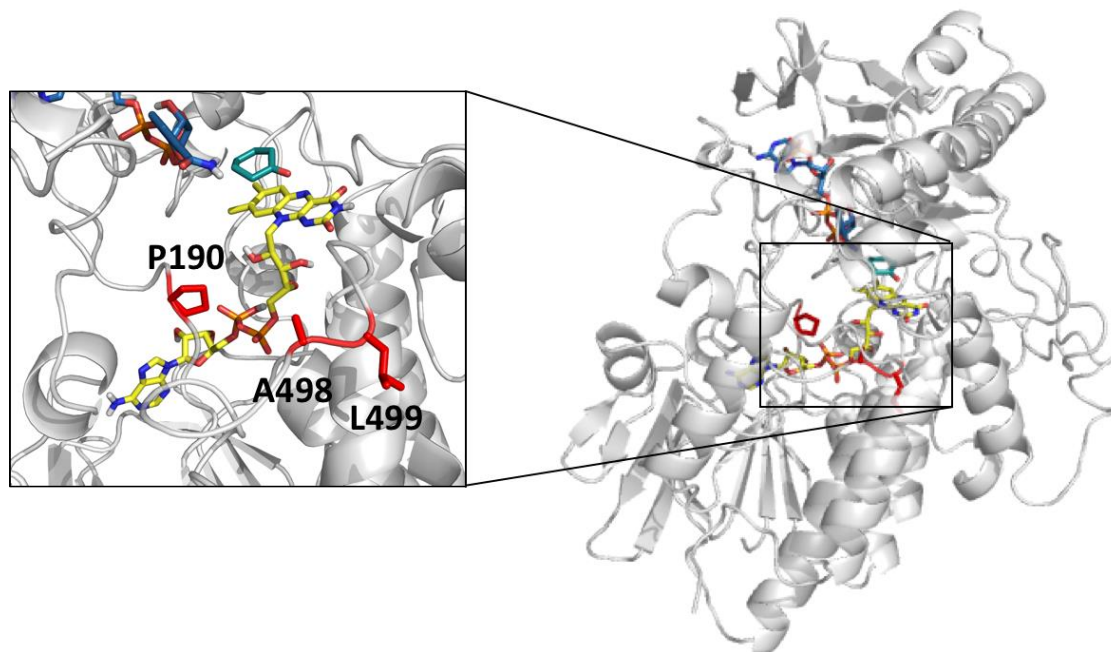
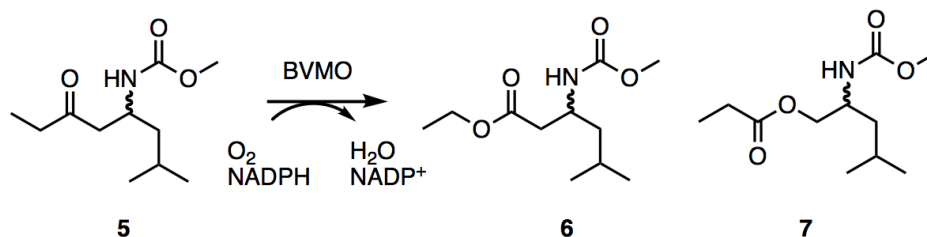


Figure 2: Homology model of CDMO. The close-up image represents the active site of the enzyme and the position of A498, L499, and P190I in regard to flavin (yellow), the substrate (green), and NADP⁺ (top left corner, blue).

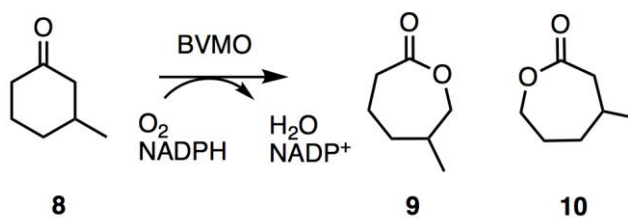
As part of our ongoing studies of CDMO regioselectivity, we chose two substrates of interest for the Baeyer-Villiger oxidation: an N-protected β -amino ketone (**5**) and 3-methylcyclohexanone (**8**). **5** can be converted into two pharmaceutically important precursors via a Baeyer-Villiger oxidation (Scheme 3). The insertion of oxygen on the less sterically hindered carbon furnishes a β -amino acid ester (**6**), which can then be hydrolyzed to its corresponding β -amino acid²⁸. The insertion of the oxygen atom at the higher substituted carbon produces β -amino alkylpropionate (**7**), which after hydrolysis can produce a β -amino alcohol. β -amino acids are building blocks of β -peptides, alkaloids, and β -lactam antibiotics while β -amino alcohols can be used as precursors for antifungal compounds²⁸⁻²⁹. The specific N-protected β -amino ketone

used in this research was methyl (2-methyl-6-oxooctan-4-yl) carbamate (**5**), which is not commercially available and was synthesized by Dr. Huanyu Zhao in the Lutz lab.



Scheme 3: BVMO-catalyzed oxidation of N-protected β -amino ketone

The second substrate of interest, 3-methylcyclohexanone (**8**) produces 5-methyl ϵ -caprolactone (**9**) and 3-methyl ϵ -caprolactone (**10**) as a result of the Baeyer-Villiger oxidation reaction (Scheme 4). The ring opening polymerization of **9** and **10** can be very useful for synthesizing biodegradable polymers³⁰. These two regioisomers give access to the polymers with distinct material properties³¹.



Scheme 4: BVMO oxidation of 3-methylcyclohexanone

2. Materials and Methods

The primers used for mutagenesis of CDMO were synthesized by Integrated DNA Technologies (Coralville, IA). All of the reagents were purchased from Sigma Aldrich (St. Louis, MO) unless otherwise specified. Sequencing was performed by Eurofins Genomics (Louisville, KY). GC spectra were obtained on an Agilent Technologies 6850 GC instrument with a chiral CycloSil-B column (30 m x 0.32 mm x 0.25 mm, Agilent, Santa Clara, CA). The carrier gas was hydrogen with the flow rate of 1.5 mL/min. The temperature of the FID detector was 250 °C with the split ratio of 50:1. GCMS spectra were obtained on a Shimadzu QP2010 SE GCMS instrument with a BGB-175 column (30 m x 0.25 mm x 0.25 mm, BGB Analytik, Alexandria, VA), and an after-column splitter. The instrument was equipped with helium a carrier gas with the flow rate of 3.69 mL/min. The split ratio was 1:1 and the temperature of the FID detector was 200 °C. MS mode EI; detector voltage 0.2 kV; mass range 12-250 u; scan speed 833 u s⁻¹.

2.1. Cloning

Mutations were introduced via overlap extension PCR using pET28a-CDMO as the template³². The forward fragment was generated using a T7 forward primer and the designed forward primer as shown in Table 1. The reverse fragment was generated using a T7 terminator primer and the designed reverse primer shown in Table 2.

PCR was performed under standard conditions using iProof High Fidelity DNA Polymerase (Bio-Rad, Hercules, CA). The PCR product and pET28a were digested at restriction sites *XbaI* and *HindIII* (New England Biolabs, Ipswich, MA). The digestion products were subsequently ligated using T4 DNA ligase (New England Biolabs). The products of ligation were

then transformed using the heat shock method into chemically competent *Escherichia coli* (*E. coli*) DH5 α cells (Invitrogen/ThermoFisher Scientific, Waltham, MA). The cells were plated on agar plates containing 30 μ g/mL kanamycin and incubated overnight at 37°C. A colony from the plate was picked to grow overnight in a 5 mL LB culture containing 50 μ g/mL kanamycin. The plasmid was then extracted from the cells via a Qiagen miniprep kit (Hilden, Germany). The mutations were then sequence confirmed.

Table 1: The sequences for the forward primers paired with T7 forward primer

Primer	Sequences
A498G Forward	5'-GGGGAATGTTCGATCCGAGACCTGCGCCCTGC-3'
L499G Forward	5'-GGGGAATGTTCGATCCGCCAGCTGCGCCCTGC-3'
A498G/L499G Forward	5'-GGGGAATGTTCGATCCGCCACCTGCGCCCTGC-3'
P190I Forward	5'-GTATGGGCACCGGCATTCTGCACGTGGCGC-3'

Table 2: The sequences for the reverse primers paired with the T7 terminator primer

Primer	Sequences
A498G Reverse	5'-GCAGGGCGCAGGTCTCGGATCGAACATTCCCC-3'
L499G Reverse	5'-GCAGGGCGCAGCTGGCGGATCGAACATTCCCC-3'
A498G/L499G Reverse	5'-GCAGGGCGCAGGTGGCGGATCGAACATTCCCC-3'
P190I Reverse	5'-GCGCCACGTGCAGAATGCCGGTGCCCATAC-3'

2.2. Expression

pET28a-CDMO or the variant plasmid, along with pGro7 (Takara Bio Inc. Japan), were cotransformed into chemically competent *E. coli* BL21(DE3) cells from Invitrogen/ThermoFisher Scientific by the heat shock method. The cells were then plated on agar plates containing 30 μ g/mL kanamycin and 34 μ g/mL chloramphenicol. After overnight incubation at 37 °C, a colony from the plate was used to inoculate 50 mL LB media supplemented with 50 μ g/mL kanamycin and 34 μ g/mL chloramphenicol. The culture was grown overnight at 37 °C, and 5 mL of it was used to inoculate 200 mL of Terrific Broth (TB) with kanamycin (50 μ g/mL), chloramphenicol (34 μ g/mL), and riboflavin (1 mM). The culture

was grown at 37 °C until the OD₆₀₀ reached 0.4–0.6, and then 2 mg/L of L-arabinose was added to induce the expression of GroEL/GroES at 20 °C. After 24 h, 0.1 mM IPTG was added to induce the expression of WT-CDMO or a CDMO variant. After 6.5 hours of incubation, the culture was centrifuged at 3,220 g at 4 °C for 30 min. The cell pellets were stored at –20 °C until purification.

2.3. Purification

WT-CDMO and CDMO variants contained an N-terminal His-tag and were purified by metal-affinity chromatography. The cell pellets were resuspended in 20 mL buffer A containing 20 µM FAD, 150 µL protease inhibitor cocktail, and 15 µL DNaseI (Calbiochem). The pellets were sonicated on ice to lyse the cells (six times, with 20-second pulses and 40-second pauses) and further centrifuged at 3,220 g and 4 °C for 1 h. All of the supernatant was loaded onto a nickel-NTA column, pre-equilibrated with buffer A (25 mM Tris-HCl at pH 7.5, 300 mM sodium chloride, 10 mM imidazole, and 1 mM β-mercaptoethanol), and incubated on a rocking table for 35 min at 4 °C. The liquid was allowed to flow through the column and was collected in a test tube. The resin was then washed twice with 5 mL of buffer A. Subsequently, resin was washed twice with 5 mL of buffer B (25 mM Tris-HCl at pH 7.5, 300 mM sodium chloride, 250 mM imidazole), followed by two 5 mL washes of buffer C (25 mM Tris-HCl at pH 7.5, 300 mM sodium chloride, 500 mM imidazole). All of the samples were collected, and an SDS-PAGE analysis was performed on the samples to determine which fractions contained the expressed protein. The ladder used was SDS-PAGE Standards, Broad Range from Bio-Rad and was used to estimate the CDMO variant with the molecular weight of 69.7 kDa. Fractions containing the protein of interest were pooled and centrifuged in Amicon Ultra-15 Centrifugal Filter (Merck

Millipore, Darmstadt, Germany) at 3,220g and 4 °C. Fractions were dialyzed twice against 2 L of buffer A to remove imidazole using dialysis tubing (10,000 MWCO, Invitrogen/ThermoFisher Scientific).

2.4. Activity Assay

Before testing the activity of the variants, enzyme concentration and extinction coefficient was determined based on the extinction coefficient of protein bound FAD. Enzyme concentration moving forward was based on the flavin-bound protein, since enzyme without flavin is inactive. Table 3 shows the values of extinction coefficients of these variants compared to the wild-type CDMO.

Three reaction mixtures were prepared for each substrate to test the activity and regioselectivity of the variant enzyme at 22 °C, 28 °C, and 34 °C. The 200 µL reaction mixture contained 100 mM glucose, 200 µM NADPH, 50 mM sodium phosphate buffer (pH 8.0), 5 U/mL glucose dehydrogenase (GDH) from *Thermoplasma acidophilum*, 2 mM enzyme, and the substrate (500 µM of **5** or 5 mM of **8**). 75 µL of the reaction was quenched in a 350 µL glass insert (Wheaton Company) with 75 µL of 0.5 mM methyl benzoate in ethyl acetate. The glass inserts were centrifuged at 2,250g for 3 min, and the organic layer was extracted into a 200 µL glass vial (VWR, Radnor, PA). GCMS was used to monitor the conversion of **5**, while GC was used to monitor the oxidation of **8**.

The primary analysis of the enzymes (herein referred to as end-point analysis) included two reaction time points: 0 h and 24 h for (*rac*)-**5**, and 0 h and 8 h for **8**. Subsequently, a time-course analysis was conducted to record the regioselectivity and conversion rate of the enzyme toward both (*rac*)-**5** and (*S*)-**5** for over 100 h. The procedure for the time-course was similar to

the end-point analysis, except the reaction was analyzed only at room temperature. The reaction time points were collected at t=0, 7, 24, 32, 50, 75, and 100 h. Note that the synthesized (*S*)-**5** contained small impurities of (*R*)-**5**, and (*rac*)-**5** was not exactly a 50:50 mixture of the two enantiomers.

Table 3: The extinction coefficients of FAD in CDMO and its constructed variants. FAD free in the solution has an absorption at 446 nm.

Enzyme	Absorption (nm)	Extinction Coefficient ($\text{mM}^{-1}\text{cm}^{-1}$)
WT-CDMO	444	13.0
A498G/L499G	443	14.8
Δ A498L499	444	16.7
A498G	443	16.2
L499G	444	15.0
P190I/A498G	445	14.0
P190I/L499G	446	13.3

2.5. GC Protocol

115 °C, hold 5 min, then 10 °C/min to 225 °C, hold for 2 min. (retention times for (*R*)-**8**. 4.8 min, (*S*)-**8**. 4.5 min **9**. 10.9 min, **10**. 11.2 min).

2.6. GCMS Protocol

110 °C, hold 15 min, then 1 °C/min to 140 °C, hold for 0.5 min. (retention times for (*R*)-**5** .38.0 min, (*S*)-**5** .38.2 min, **6**. 41.5 min, **7**. 36.3 min).

3. Results and Discussion

3.1. Loop Mutations

A498G/L499G, Δ A498L499, A498G, and L499G were among the first variants of CDMO constructed and analyzed. A sample SDS-PAGE analysis of A498G is shown in Figure 3. Overall, all of the mentioned variants were soluble and eluted off of the metal affinity column as the concentration of imidazole in the buffer increased. The last four lanes in Figure 3 show the presence of the protein bands corresponding with the molecular weight of the CDMO variant (approximately 69.7 kDa).

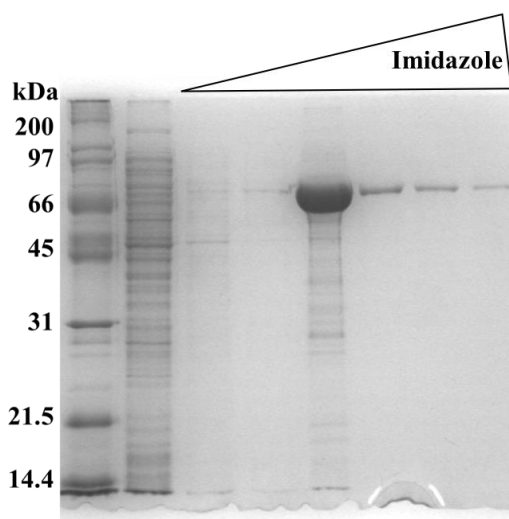


Figure 3: SDS-PAGE Gel of A498G variant. From left to right: ladder, flow-through, two lanes for first and second washes with buffer A, two lanes for first and second washes with buffer B, and two lanes for first and second washes with buffer C.

In the initial end-point analysis, all of the variants exhibited activity towards both substrates, except variant Δ A498L499 which showed little to no activity. Table 4 and 5 represent the activity and regioselectivity of each of these variants towards substrate **5** and **8**, respectively. The fold activity values in the table are in comparison with the WT-CDMO values at the corresponding temperature. Note that the reactions did not necessarily proceed to completion,

and thus, the ratio of products shown in the tables are in relation to the average percent conversion of substrate within the reaction time.

Table 4: End-point analysis of WT-CDMO and the loop variants with substrate **5**. The values are in relation to product formation after 24 hours.

Enzyme	Temperature (°C)	Average % Conversion of 5	Standard Deviation	Fold Activity	Ratio of 6:7
WT-CDMO	22	9.9%	0.2%	1.0	54:46
WT-CDMO	28	17.2%	0.3%	1.0	60:40
WT-CDMO	34	26.9%	1.0%	1.0	62:37
A498G/L499G	22	4.3%	0.3%	0.4	64:36
A498G/L499G	28	8.9%	3.2%	0.5	70:30
A498G/L499G	34	6.6%	1.8%	0.2	73:27
A498G	22	12.0%	0.7%	1.2	75:25
A498G	28	24.3%	0.7%	1.4	81:19
A498G	34	35.0%	1.3%	1.3	85:15
L499G	22	40.0%	1.1%	4.0	82:18
L499G	28	46.1%	0.6%	2.7	82:18
L499G	34	27.7%	1.6%	1.0	89:11
Δ 498499	22	0.6%	0.0%	0.1	67:33
Δ 498499	28	0.1%	0.0%	0.0	Unable to Detect
Δ 498499	34	0.2%	0.0%	0.0	Unable to Detect

Table 5: End-point analysis of WT-CDMO and the loop variants with substrate **8**. The values are in relation to product formation after 8 hours.

Enzyme	Temperature (°C)	Average % Conversion of 8	Standard Deviation	Fold Activity	Ratio of 9:10
WT-CDMO	22	15.6%	0.3%	1.0	74:26
WT-CDMO	28	19.7%	1.2%	1.0	74:26
WT-CDMO	34	24.7%	0.3%	1.0	73:27
A498G/L499G	22	11.1%	0.3%	0.7	75:25
A498G/L499G	28	17.7%	0.6%	0.9	76:24
A498G/L499G	34	13.2%	0.4%	0.5	79:21
A498G	22	16.0%	0.3%	1.0	76:24
A498G	28	19.1%	0.3%	1.0	75:25
A498G	34	13.1%	0.3%	0.5	78:22
L499G	22	18.0%	0.3%	1.2	76:24
L499G	28	15.5%	5.9%	0.8	66:34
L499G	34	15.8%	0.4%	0.6	79:21
Δ498499	22	0.0%	0.0%	0.0	0:0
Δ498499	28	0.0%	0.0%	0.0	0:0
Δ498499	34	0.0%	0.0%	0.0	0:0

WT-CDMO shows higher percentage of substrate conversion at elevated temperatures.

The greater activity of WT-CDMO for its enzymatic reactions at 34 °C suggests that this enzyme retains stability at these elevated temperatures. Only variant A498G shows a similar trend in the presence of substrate **5**, while in other cases, the variants do not favor high temperature.

Furthermore, the data suggests that substitutions in the arginine-interacting loop generally results in a higher regioselectivity of the enzyme towards product **6**. Variants A498G and L499G showed enhanced activity compared to WT-CDMO, with an average fold activity of 1.3 and 2.6, respectively. Combination of those two substitutions, as seen in variant A498G/L499G,

diminished the activity of the enzyme and did not significantly alter its regioselectivity. In contrast, neither of the loop variants showed significant change towards substrate **8**. This indicates that the loop substitutions were not creating a suitable active site for this substrate to gain higher activity or to affect regioselectivity.

Variants A498G and L499G were selected for time-course analysis due to their interesting initial results towards **5**. Two separate time-course reactions were conducted for each variant, one with (*rac*)-**5** and another with chiral (*S*)-**5**. Due to limitations of the current analytical method, we are unable to separate the enantiomers of **6** and **7**. Therefore, we follow the consumption of (*R*)-**5** and (*S*)-**5** and monitor the regioisomer formed to identify the enantiomer of each regioisomer. The reaction with (*rac*)-**5** determined the enzyme's enantiomeric preference for the substrate (Figure 4). The reaction with (*S*)-**5** helped us to identify the regioisomer formed from the consumption of this enantiomer (Figure 5). This time-course analysis was conducted at 22 °C.

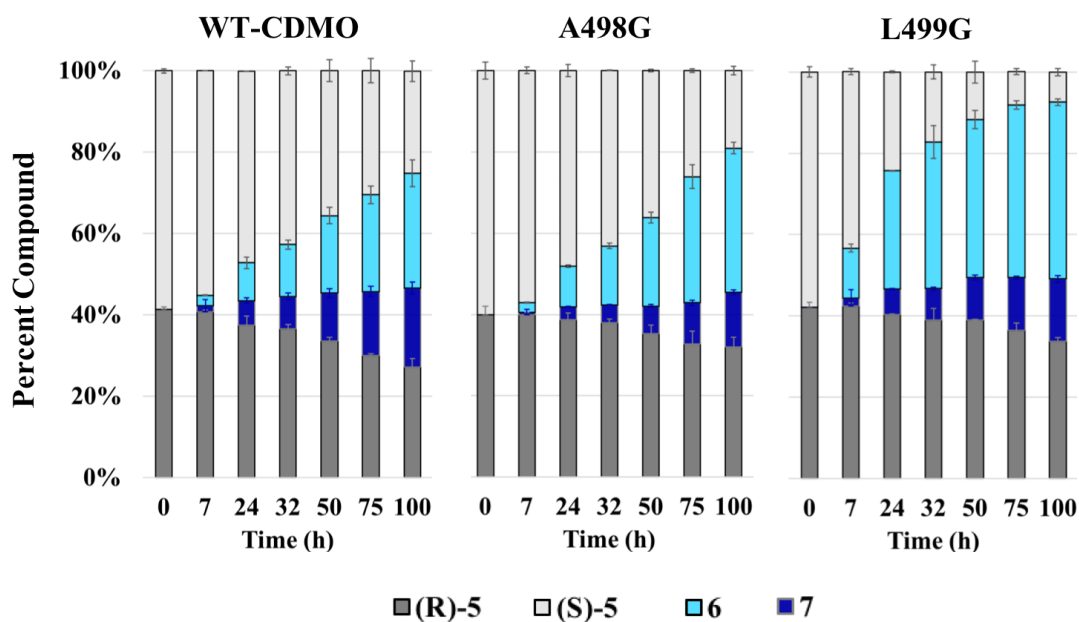


Figure 4: Time-course analysis of WT-CDMO and variants A498G and L499G with (*rac*)-**5** conducted at 22 °C.

Looking at the results in Figure 4, we hypothesize that the loop variants consume the (*R*)-enantiomer to produce **7** and convert the (*S*)-enantiomer to **6**. When given the racemic mixture of **5**, variants A498G and L499G show a clear preference for the (*S*)-**5**. The consumption of this enantiomer is directly proportional to production of **6**. Within the first 50 hours of the reaction, A498G and WT-CDMO show roughly a similar substrate conversion to **6**. In the final 50 hours, however, A498G shows greater preference for (*S*)-**5** and yielded a higher ratio of **6**. Moreover, only when a small amount of (*S*)-**5** is left does variant L499G start to consume (*R*)-**5** (as seen at 75 h, Figure 4).

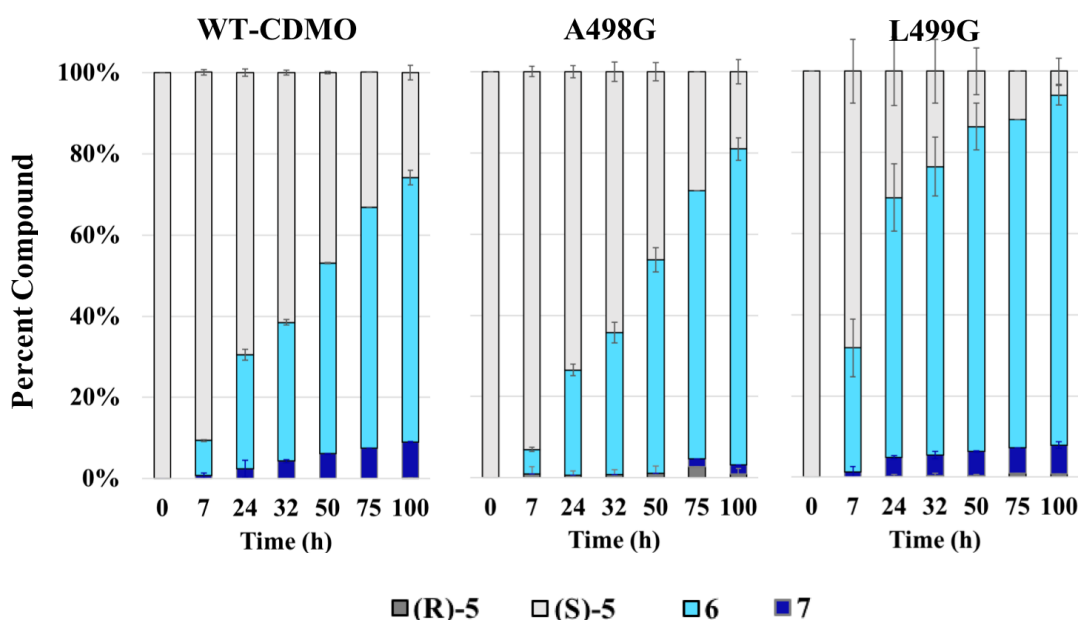


Figure 5: Time-course analysis of WT-CDMO and variants A498G and L499G with (*S*)-**5** conducted at 22 °C.

Our hypothesis about the conversion of (*S*)-**5** to **6** is supported by the data in Figure 5. The small amount of **7** produced in those reactions is more likely linked to the impurity of the starting material, as discussed in the Methods and Materials section. While 75 hours is required for WT-CDMO to use roughly 60% of the (*S*)-enantiomer, it only takes 24 hours for L499G to

reach a similar level of conversion. Being able to conduct what was a three-day reaction in one day can be tremendously beneficial in the industrial setting.

As many of the previous BVMO engineering works gained additive results by coupling mutations of different regions, I sought opportunities to do the same. Dr. Leann Teadt had previously worked on a number of mutations in different residues to alter the regioselectivity of CDMO. A promising variant constructed by her was P190I. While this variant was highly regioselective towards **6**, it showed greatly diminished catalytic activity relative to WT-CDMO. The results of the end-point analyses of this variant are shown in Table 6 and 7. We aimed to see if constructing variants, P190I/A498G and P190I/L499G, would regain the activity seen with A498G and L499G variants, but have the high regioselectivity of the P190I variant.

3.2. Variants P190I/A498G and P190I/L499G

End-point analyses were conducted with variants P190I/A498G and P190I/L499G, and the results with substrate **5** and **8** are shown in Table 6 and 7, respectively. Variant P190I/A498G showed decent thermal stability and was more selective towards **6** and **9** as the temperature increased. P190I/L499G was selective towards **6**, producing 92:8 of **6:7**, and demonstrated significant fold activity at 22 °C. While the results were very promising for conversion of **5**, no significant change was observed with **8**.

Table 6: 24 h time-point analysis of P190I, P190I/A498G, and P190I/L499G with substrate **5**. The values are in relation to product formation after 24 hours.

Enzyme	Temperature (°C)	Average % Conversion of 5	Standard Deviation	Fold Activity	Ratio of 6:7
WT-CDMO	22	9.9%	0.2%	1.0	54:46
WT-CDMO	28	17.2%	0.3%	1.0	60:40
WT-CDMO	34	26.9%	1.0%	1.0	62:37
P190I	22	7.4%	0.4%	0.7	85:15
P190I	28	15.2%	1.6%	0.9	83:17
P190I	34	27.4%	0.8%	1.0	82:18
P190I/A498G	22	54.1%	7.5%	5.5	88:12
P190I/A498G	28	59.2%	0.1%	3.4	88:12
P190I/A498G	34	58.3%	1.5%	2.2	90:10
P190I/L499G	22	54.7%	1.0%	5.5	92:8
P190I/L499G	28	53.8%	0.3%	3.1	88:12
P190I/L499G	34	43.5%	0.7%	1.6	93:7

Table 7: 8 h time-point analysis of P190I, P190I/A498G, and P190I/L499G with substrate **8**. The values are in relation to product formation after 8 hours.

Enzyme	Temperature (°C)	Average % Conversion of 8	Standard Deviation	Fold Activity	Ratio of 9:10
WT-CDMO	22	15.6%	0.3%	1.0	74:26
WT-CDMO	28	19.7%	1.2%	1.0	74:26
WT-CDMO	34	24.7%	0.3%	1.0	73:27
P190I	22	16.0%	0.6%	1.0	58:42
P190I	28	22.3%	0.9%	1.1	59:41
P190I	34	31.8%	2.6%	1.3	61:39
P190I/A498G	22	14.4%	0.2%	0.9	60:40
P190I/A498G	28	16.0%	1.5%	0.8	62:38
P190I/A498G	34	18.1%	0.6%	0.7	68:32
P190I/L499G	22	14.4%	0.5%	0.9	65:35
P190I/L499G	28	16.1%	1.4%	0.8	67:33
P190I/L499G	34	11.6%	9.0%	0.5	71:29

The two double-substituted variants were further tested in time-course reactions with both (*Rac*)-**5** and (*S*)-**5**. Figure 6 shows the high preference of both of the variants for consumption of (*S*)-**5**. P190I/A498G consumes less than half of (*R*)-**5** provided in the solution but does not convert it all to **7**. In the absence of further experiments with the chirally pure (*R*)-**5**, we hypothesize that P190I/A498G is capable of converting (*R*)-**5** to both regioisomers. Additionally, P190I/L499G strictly relies on the (*S*)-enantiomer and consumes all of it within the first 50 hours. This high consumption is also observed in the results shown in Figure 7, where P190I/L499G has less than 2% of the (*S*)-enantiomer left after 50 h. Both of the variants are more efficient for the production of **6** compared to the WT-CDMO.

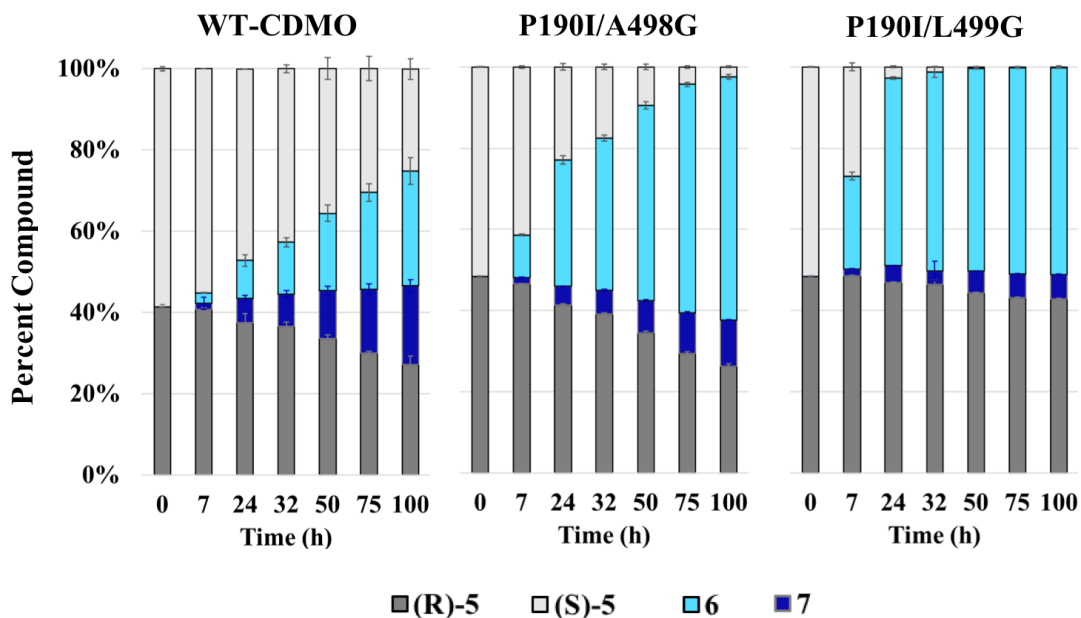


Figure 6: Time-course analysis of WT-CDMO and variants P190I/A498G and P190I/L499G with (*rac*)-**5** conducted at 22 °C.

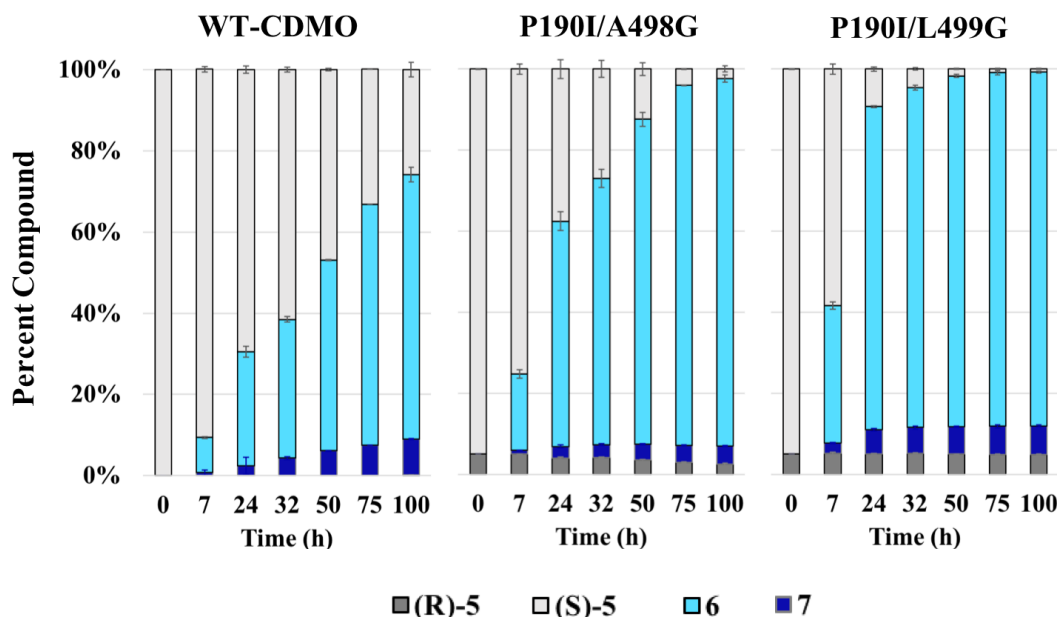


Figure 7: Time-course analysis of WT-CDMO and variants P190I/A498G and P190I/L499G with (*S*)-**5** conducted at 22 °C.

While the substitutions in the arginine-interacting loop resulted in greater activity of the enzyme towards **5**, that may not be the case for all substrates. The active site of these variants

may show an optimal catalytic space for one substrate whereas with another substrate it may not fit and subsequently show low or no activity. The preferred active site residues for each substrate is different depending on the substrate's size, shape, and charge distribution. This claim can be supported by comparing data from the reactions of CDMO variants with **5** and **8**. Specifically, P190I/A498G and P190I/L499G were each 5.5 folds more active towards **5** than WT-CDMO and demonstrate enhanced regioselectivity. The same variants, however, showed poor activity towards **8** and presented lower regioselectivity than the wild-type enzyme. WT-CDMO has an enlarged active site and therefore is better suited to accept substrates with extended carbon-chains. Further opening up the active site was not effective for increasing the activity and regioselectivity of **8**, as seen for variants A498G/L499G, A498G, and L499G.

Truncation of amino acid side chains on the loop enlarged and shifted the active site of the enzyme. The position of the substrate was therefore altered, which resulted in enhanced regioselectivity of the variant towards **6**. Presumably, when the substrate benefited from more space by the loop, it allowed the migratory bond in the Criegee intermediate to position itself in a way that favored the production of **6**. Additionally, P190 is located directly across from the loop (Figure 8) and substituting this residue to isoleucine reorganizes the active site away from this region. However, this substitution crowded the substrate in the active site and led to the poor activity of the variant. The combinations of the loop's single substitution with P190I seemed to compensate for these effects and presumably locking the substrate in a catalytically relevant position to create a stable Criegee intermediate in which the migratory group favored the production of **6**.

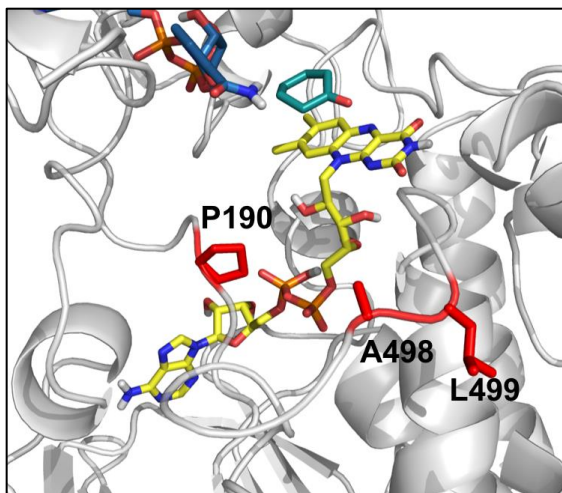


Figure 8: The homology model showing the active site of CDMO with the key residues P190I, A498G, and L499G (red). The loop residues are across from P190I, and these residues play an important role in the positioning of Criegee intermediate formed from **5**.

4. Conclusion

To better compare the activity and regioselectivity of the variants, the end-point analyses for substrate **5**, obtained at 22 °C, are illustrated in Figure 9. The data from the P190I variant (obtained by Dr. Leann Teadt) and the loop's single variants allow for better visualization of the improvement of P190I/A498G and P190I/L499G. Coupling the single amino acid substitutions of CDMO's arginine-interacting loop with P190I successfully shifted the enzyme's active site, leading to an increased rate of conversion and regioselectivity towards **6**. The repositioning of the substrate away from residue 190 and closer to the loop's backbone enabled the enzyme to gain activity and show preference for **6**. This regioisomer is produced from insertion of the oxygen atom in the less substituted carbon chain, and therefore, it is considered the unnatural product of the chemical Baeyer-Villiger reaction.

In previous experiments on BVMOs, such as the one performed by the Bornscheuer group, the activity of the enzyme was negatively affected as a result of a switch in regioselectivity¹⁴. The work presented in this thesis, however, resulted in regioselectivity up to 92% towards **6** at 22 °C (P190I/L499G) with a fold activity increase of 5.5 relative to WT-CDMO. Here we introduce novel variants of CDMO with greater activity and regioselectivity that favor the production of **6**, which is the building block of β -peptides, alkaloids, and β -lactam antibiotics²⁸.

The future work of this project will focus on separating the enantiomers of **6** and **7** via derivatization to confirm that the enantiomer of the substrate consumed is linked with the enantiomer of the product formed. This information will tell us more about the interaction of the selected active site residues with the substrate. Furthermore, additional attempts to obtain a

crystal structure of CDMO would allow us to rationalize the data in this experiment with a higher degree of certainty.

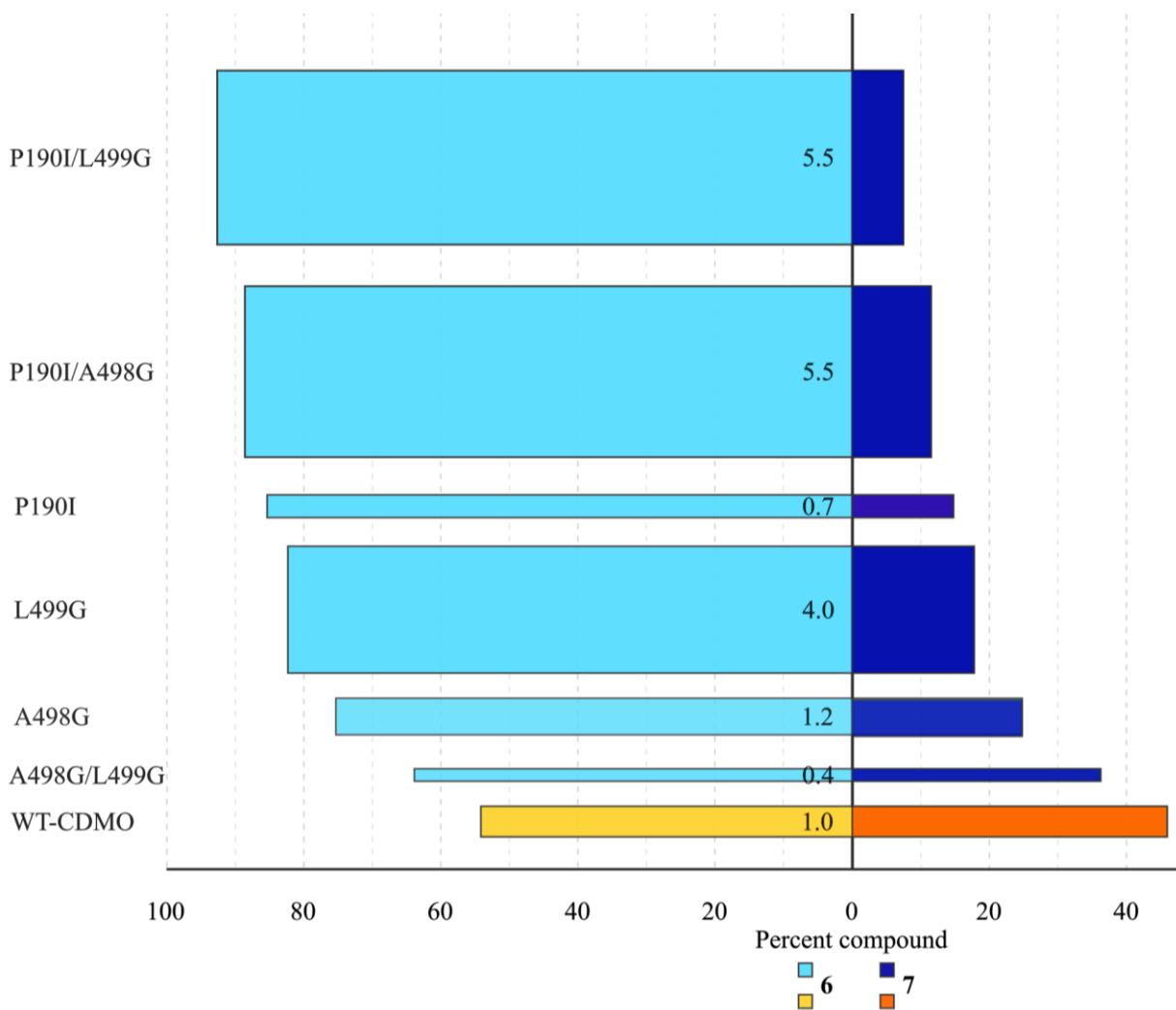


Figure 9: Time-point analysis of WT-CDMO (shown in yellow and orange), P190I, and the variants containing mutations in the arginine-interacting loop with substrate **5**. The thickness of the bars represents the activity of the enzyme in comparison with WT-CDMO, with the fold activities indicated by the numbers. The left side of the graph (light blue and yellow) represent the percent conversion to **6**, and the right side (dark blue and orange) represent the percent conversion to product **7**.

5. References

1. Krow, G. R., The Baeyer–Villiger oxidation of ketones and aldehydes. *Organic Reactions* **1993**.
2. Świzdor, A., Baeyer-Villiger oxidation of some C19 steroids by *Penicillium lanosocoeruleum*. *Molecules* **2013**, *18* (11), 13812-13822.
3. Baeyer, A.; Villiger, V., Einwirkung des Caro'schen Reagens auf Ketone. *Berichte der deutschen chemischen Gesellschaft* **1899**, *32* (3), 3625-3633.
4. Criegee, R., Die Umlagerung der Dekalin-peroxydester als Folge von kationischem Sauerstoff. *Eur. J. Org. Chem.* **1948**, *560* (1), 127-135.
5. Leisch, H.; Morley, K.; Lau, P. C. K., Baeyer–Villiger Monooxygenases: More Than Just Green Chemistry. *Chem. Rev.* **2011**, *111* (7), 4165-4222.
6. Renz, M.; Meunier, B., 100 Years of Baeyer–Villiger Oxidations. *Eur. J. Org. Chem.* **1999**, (4), 737-750.
7. Chi, J.-H.; Wu, S.-H.; Shu, C.-M., Thermal explosion analysis of methyl ethyl ketone peroxide by non-isothermal and isothermal calorimetric applications. *J. Hazard. Mater.* **2009**, *171* (1), 1145-1149.
8. Balke, K.; Kadow, M.; Mallin, H.; Sa; Bornscheuer, U. T., Discovery, application and protein engineering of Baeyer-Villiger monooxygenases for organic synthesis. *Org. Biomol. Chem.* **2012**, *10* (31), 6249-6265.
9. Balke, K.; Beier, A.; Bornscheuer, U. T., Hot spots for the protein engineering of Baeyer-Villiger monooxygenases. *Biotechnol. Adv.* **2017**.
10. Willetts, A., Structural studies and synthetic applications of Baeyer-Villiger monooxygenases. *Trends Biotechnol.* **1997**, *15* (2), 55-62.
11. Mihovilovic, Marko D.; Müller, B.; Stanetty, P., Monooxygenase-Mediated Baeyer–Villiger Oxidations. *Eur. J. Org. Chem.* **2002**, (22), 3711-3730.
12. Sheng, D.; Ballou, D. P.; Massey, V., Mechanistic Studies of Cyclohexanone Monooxygenase: Chemical Properties of Intermediates Involved in Catalysis. *Biochemistry* **2001**, *40* (37), 11156-11167.
13. Mirza, I. A.; Yachnin, B. J.; Wang, S.; Grosse, S.; Bergeron, H.; Imura, A.; Iwaki, H.; Hasegawa, Y.; Lau, P. C. K.; Berghuis, A. M., Crystal Structures of Cyclohexanone Monooxygenase Reveal Complex Domain Movements and a Sliding Cofactor. *J. Am. Chem. Soc.* **2009**, *131* (25), 8848-8854.
14. Balke, K.; Schmidt, S.; Genz, M.; Bornscheuer, U. T., Switching the Regioselectivity of a Cyclohexanone Monooxygenase toward (+)-trans-Dihydrocarvone by Rational Protein Design. *ACS Chem. Biol.* **2016**, *11* (1), 38-43.
15. Donoghue, N. A.; Norris, D. B.; Trudgill, P. W., The Purification and Properties of Cyclohexanone Oxygenase from *Nocardia globerulea* CL1 and *Acinetobacter* NCIB 9871. *Eur. J. Biochem.* **1976**, *63* (1), 175-192.
16. Pazmiño, D. E. T.; Snajdrova, R.; Rial, D. V.; Mihovilovic, M. D.; Fraaije, M. W., Altering the Substrate Specificity and Enantioselectivity of Phenylacetone Monooxygenase by Structure-Inspired Enzyme Redesign. *Adv. Synth. Catal.* **2007**, *349* (8-9), 1361-1368.
17. Bocola, M.; Schulz, F.; Leca, F.; Vogel, A.; Fraaije, M. W.; Reetz, M. T., Converting Phenylacetone Monooxygenase into Phenylcyclohexanone Monooxygenase by Rational Design: Towards Practical Baeyer–Villiger Monooxygenases. *Adv. Synth. Catal.* **2005**, *347* (7-8), 979-986.

18. Yachnin, B. J.; McEvoy, M. B.; MacCuish, R. J. D.; Morley, K. L.; Lau, P. C. K.; Berghuis, A. M., Lactone-Bound Structures of Cyclohexanone Monooxygenase Provide Insight into the Stereochemistry of Catalysis. *ACS Chem. Biol.* **2014**, *9* (12), 2843-2851.
19. Malito, E.; Alfieri, A.; Fraaije, M. W.; Mattevi, A., Crystal structure of a Baeyer–Villiger monooxygenase. *Proc. Natl. Acad. Sci. U. S. A.* **2004**, *101* (36), 13157-13162.
20. Reetz, M. T.; Wu, S., Greatly reduced amino acid alphabets in directed evolution: making the right choice for saturation mutagenesis at homologous enzyme positions. *Chem. Commun.* **2008**, (43), 5499-5501.
21. Dudek, H. M.; de Gonzalo, G.; Pazmiño, D. E. T.; Stepniak, P.; Wyrwicz, L. S.; Rychlewski, L.; Fraaije, M. W., Mapping the substrate binding site of phenylacetone monooxygenase from *Thermobifida fusca* by mutational analysis. *Appl. Environ. Microbiol.* **2011**, *77* (16), 5730-5738.
22. Fink, M. J.; Rial, D. V.; Kapitanova, P.; Lengar, A.; Rehdorf, J.; Cheng, Q.; Rudroff, F.; Mihovilovic, M. D., Quantitative Comparison of Chiral Catalysts Selectivity and Performance: A Generic Concept Illustrated with Cyclododecanone Monooxygenase as Baeyer–Villiger Biocatalyst. *Adv. Synth. Catal.* **2012**, *354* (18), 3491-3500.
23. Kostichka, K.; Thomas, S. M.; Gibson, K. J.; Nagarajan, V.; Cheng, Q., Cloning and characterization of a gene cluster for cyclododecanone oxidation in *Rhodococcus ruber* SC1. *J. Bacteriol.* **2001**, *183* (21), 6478-6486.
24. Orru, R.; Balke, K.; Bornscheuer, U. T.; Lutz, S., Catalytic and Kinetic Properties of Cyclododecanone Monooxygenase from *Rhodococcus Ruber* SC1
. **To be submitted**
25. Fürst, M. J.; Savino, S.; Dudek, H. M.; Gómez Castellanos, J. R. b.; Gutiérrez de Souza, C.; Rovida, S.; Fraaije, M. W.; Mattevi, A., Polycyclic ketone monooxygenase from the thermophilic fungus *Thermothelomyces thermophila*: A structurally distinct biocatalyst for bulky substrates. *J. Am. Chem. Soc.* **2017**, *139* (2), 627-630.
26. Källberg, M.; Wang, H.; Wang, S.; Peng, J.; Wang, Z.; Lu, H.; Xu, J., Template-based protein structure modeling using the RaptorX web server. *Nat. Protoc.* **2012**, *7* (8), 1511.
27. Leaver-Fay, A.; Tyka, M.; Lewis, S. M.; Lange, O. F.; Thompson, J.; Jacak, R.; Kaufman, K. W.; Renfrew, P. D.; Smith, C. A.; Sheffler, W., ROSETTA3: an object-oriented software suite for the simulation and design of macromolecules. In *Methods Enzymol.*, Elsevier: 2011; Vol. 487, pp 545-574.
28. Juaristi, E.; Soloshonok, V. A., *Enantioselective synthesis of beta-amino acids*. John Wiley & Sons: 2005.
29. Ager, D. J.; Prakash, I.; Schaad, D. R., 1,2-Amino Alcohols and Their Heterocyclic Derivatives as Chiral Auxiliaries in Asymmetric Synthesis. *Chem. Rev.* **1996**, *96* (2), 835-876.
30. Gross, R. A.; Kalra, B., Biodegradable polymers for the environment. *Science* **2002**, *297* (5582), 803-807.
31. Messiha, H. L.; Ahmed, S. T.; Karuppiah, V.; Suardiaz, R.; Ascue Avalos, G. A.; Fey, N.; Yeates, S.; Toogood, H. S.; Mulholland, A. J.; Scrutton, N. S., Biocatalytic Routes to Lactone Monomers for Polymer Production. *Biochemistry* **2018**.
32. Heckman, K. L.; Pease, L. R., Gene splicing and mutagenesis by PCR-driven overlap extension. *Nat. Protoc.* **2007**, *2* (4), 924.